

Density Functional Theory Analysis of Stereoelectronic Properties of Cobalamins[†]Tadeusz Andruniow,⁺ Marek Z. Zgierski,[‡] and Pawel M. Kozlowski^{*,+}*Department of Chemistry, University of Louisville, Louisville, Kentucky 40292, and Steacie Institute for Molecular Science, National Research Council of Canada, Ottawa, Ontario, Canada K1A 0R6**Received: March 1, 2000; In Final Form: September 7, 2000*

Density functional theory (DFT) is applied to the calculation of the steric and electronic factors which might affect the Co–C_R bond activation in coenzyme B₁₂. The six-coordinate cobalamins (B–[Co^{III}(corrin)]–R, models of coenzyme B₁₂) include the actual corrin macrocoring as the equatorial ligand and imidazole (Im), dimethylbenzimidazole (DBI) or water (H₂O), as the α-trans ligand (B). The β axial ligand (R) represents a series of alkyl groups with different steric bulkiness ranging from –C≡N, –C≡CH through methyl, ethyl, isopropyl, *tert*-butyl to 5'-deoxy-5'-adenosyl. Each trans ligand (Im, DBI or H₂O) produces a positive correlation of the Co–C_R and Co–N_B bond lengths. The increasing complexity of the R group leads to two major structural correlations: a positive correlation between the Co–C_R and Co–N_B bond lengths and an inverse correlation between the Co–C_R bond length and the flatness of the corrin ring. It is shown that stereoelectronic properties of cobalamins can only be explained on the basis of electronic considerations. Moreover, electron donation from axial ligands to the cobalt atom either by electron donating substituents or by a properly oriented external electric field caused by external electric charges is argued to be the main trigger for the activation of the Co–C_R bond.

Introduction

The catalytic activation of the Co–C_R bond of coenzyme B₁₂ (Figure 1) has been both a key problem and a major dispute in B₁₂ chemistry.¹ The apoenzymes that bind and utilize the coenzyme must act to mitigate, to a surprising extent, the inherent kinetic inertness of the Co–C_R bonds. The degree of Co–C_R bond activation is spectacular, since the Co–C_R bond is ordinarily quite stable. The Co–C_R dissociation enthalpy is 31.5 ± 2 kcal/mol for 5'-deoxy-5'-adenosyl-cobalamine [AdoCbl] and the thermal homolysis rate at 25 °C is only 4 × 10^{−10} s^{−1}.² In AdoCbl dependent enzymes this rate is increased by a factor of 10^{12±1}, implying a ~15 kcal/mol destabilization of the Co–C_R bond.³ Precisely how such tremendous acceleration is achieved and controlled is a topic of intense interest but is not adequately understood at present. Research in this field has suggested several mechanisms,⁴ but none can be considered as fully satisfactory in light of a large body of experimental results.^{4c,5} The most frequently proposed mechanism involves steric interaction of the cofactor with the protein matrix, while electronic factors have usually been considered less important. The flexibility of the corrin macrocycle ring,⁶ the angular distortion of the alkyl group⁷ and the displacement of the axial base ligand⁸ have been proposed as key variables in the conformational distortion picture.

The aim of the present paper is to investigate the stereoelectronic factors, which might affect the Co–C_R bond length in B₁₂-dependent enzymes using density functional theory (DFT). Recent advances in computational power, coupled with important theoretical developments in modern DFT, give increased confidence in the reliability and applicability of theoretical methods to elucidate the electronic structure and spectroscopic properties of transition metal systems including the active sites

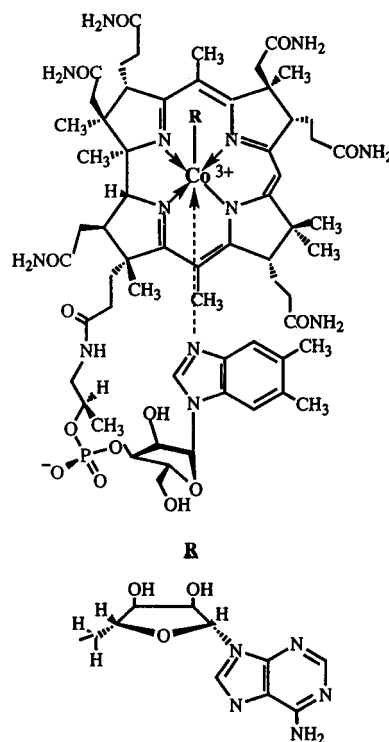


Figure 1. Molecular structure of 5'-deoxy-5'-adenosyl-cobalamine [coenzyme B₁₂].

of metalloenzymes.⁹ Computational chemistry is now emerging as a powerful tool to understand these bioinorganic systems. Evaluation of possible factors affecting the bond catalytic activation of the Co–C_R bond in coenzyme B₁₂ has only been carried out for simplified model systems, especially for corrin.^{7b,8a,10,11a} To date, only two theoretical studies have appeared on such a model^{7b,11b} and only one included optimized geometries.^{11b} Therefore, there is a need for high-quality

[†] Part of the special issue "Thomas Spiro Festschrift".

⁺ University of Louisville.

[‡] National Research Council of Canada.

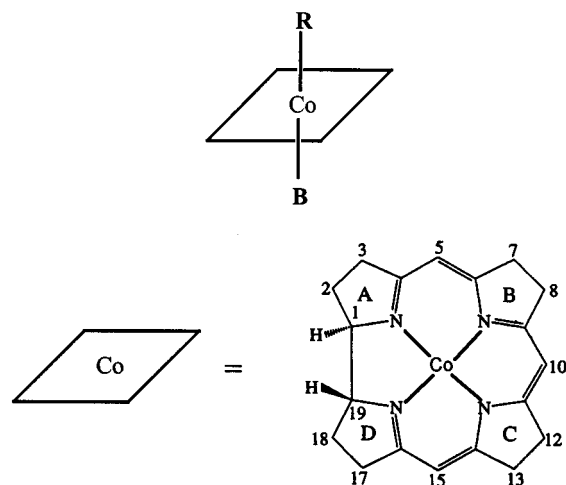


Figure 2. Molecular structure of model cobalamins. β -Axial ligands: R = $-\text{C}\equiv\text{N}$ ($-\text{CN}$), $-\text{C}\equiv\text{CH}$ ($-\text{CCH}$), methyl ($-\text{Me}$), ethyl ($-\text{Et}$), isopropyl ($-\text{iProp}$), *tert*butyl ($-\text{tBut}$), 5'-deoxy-5'-adenosyl ($-\text{Ado}$). α -Trans ligands: B = Im (imidazole), DBI (dimethylbenzimidazole), H_2O (water).

theoretical studies using more realistic corrin-based coenzyme B_{12} model. Preliminary results of this work has been published elsewhere.¹²

Computational Methods

Calculations were carried out using gradient-corrected DFT with the Becke–Lee–Yang–Parr composite exchange correlation functional (B3LYP). The B3LYP level of theory with 6-31G (d) [for H, C, N] and Ahlrich's VTZ [for Co]¹³ basis sets, successfully used in previous calculations on metalloporphyrins,¹⁴ were employed in the present study. All calculations were carried out with the Gaussian98^{15a} and PQS^{15b} suite of programs for electronic structure calculations. The six-coordinate cobalamin models, $\text{B}-[\text{Co}^{\text{III}}(\text{corrin})]-\text{R}$, investigated in the present work include the actual corrin macrocycle ring as the equatorial ligand system and imidazole (Im), dimethylbenzimidazole (DBI) or water (H_2O) base as the α -trans ligand. The sidearm and peripheral substituents of the corrin ring (Figure 1) were left out to simplify the calculations while still retaining the important structural features (Figure 2). The β axial ligand was modeled by a series of groups with different steric sizes ranging from $-\text{C}\equiv\text{N}$ ($-\text{CN}$), $-\text{C}\equiv\text{CH}$ ($-\text{CCH}$), through methyl (Me), ethyl (Et), isopropyl (iProp), *tert*-butyl (tBut), to 5'-deoxy-5'-adenosyl (Ado) (Figure 2).

Results and Discussion

The objective of the present work was to investigate the steric and electronic factors, which might affect the $\text{Co}-\text{C}_\text{R}$ bond in coenzyme B_{12} . To accomplish this, the molecular structures of $\text{B}-[\text{Co}^{\text{III}}(\text{corrin})]-\text{R}$ complexes, for a range of bases B and alkyl R ligands (Figure 2), were fully optimized and the results scrutinized with respect to the optimized structural parameters. Analysis of the optimized cobalamin structural parameters (full list in the Supporting Information) shows that only two bond lengths, $\text{Co}-\text{C}_\text{R}$ and $\text{Co}-\text{N}_\text{B}$, and eight torsional angles were affected by variation of the B and R groups, while the majority of structural parameters associated with the corrin ring remained essentially unchanged. This observation is consistent with the fact that cobalamin crystal structures tend to be similar.²⁰ Analysis of the selected DFT optimized parameters of $\text{B}-[\text{Co}^{\text{III}}-$

(corrin)]-R complexes (Tables 1–4) shows that models with DBI base and $-\text{CN}$ or $-\text{Me}$ alkyl ligands are in much better agreement with experimental data for vitamin B_{12} wet¹⁷ (dry)¹⁸ and MeB_{12} ¹⁹ (Tables 2 and 4) than for the structure of $\text{Im}-[\text{Co}^{\text{III}}(\text{corrin})]-\text{CN}$ compared with $\text{Co}\beta$ -cyanoimidazolylcobamide.¹⁶ The latter structure is not well reproduced by our calculations. The equatorial $\text{Co}-\text{N}[1,2,3,4]$ bond lengths tend to be overestimated by 0.069, 0.051, 0.098, and 0.015 Å, respectively, while the $\text{Co}-\text{N}_\text{B}$ bond length difference is about 0.122 Å. The agreement is better for $\text{DBI}-[\text{Co}^{\text{III}}(\text{corrin})]-\text{CN}$ compared with dry vitamin B_{12} ¹⁸ where the $\text{Co}-\text{N}[1,2,3,4]$ bond length difference is about ~ 0.045 Å (an average) and quite excellent for $\text{DBI}-[\text{Co}^{\text{III}}(\text{corrin})]-\text{Me}$ in comparison with MeB_{12} ,¹⁹ not only in terms of the selected optimized bond lengths, i.e., equatorial $\text{Co}-\text{N}[1,2,3,4] \sim 0.012$ Å (in average) and $\text{Co}-\text{C}_\text{R}$ 0.28 Å (Table 2), but also in terms of bond angles (Table 4). However, our calculations do not reproduce well the $\text{Co}-\text{N}_\text{B}$ bond distance and for two of the investigated structures the discrepancy is in range of 0.1 Å. The nature of these discrepancies lies in the shallowness of the potential energy surface with respect to $\text{Co}-\text{N}_\text{B}$ stretch. The difference between the calculated and experimental bond distances could be due to errors in the calculations, experiments or both. Although the difference between the calculated and experimental bond lengths cannot be ruled out on energetic grounds, we cannot explain why $\text{Im}-[\text{Co}^{\text{III}}(\text{corrin})]-\text{CN}$ differs significantly from $\text{Co}\beta$ -cyanoimidazolylcobamide.¹⁶

The increased complexity of the R group produces two major structural correlations: a positive linear correlation between the $\text{Co}-\text{C}_\text{R}$ and $\text{Co}-\text{N}_\text{B}$ bond lengths and an inverse correlation between the $\text{Co}-\text{C}_\text{R}$ bond length and flatness of the corrin ring. The positive correlation between the two axial bond lengths in the $\text{N}_\text{B}-\text{Co}-\text{C}_\text{R}$ moiety is similar to a correlation obtained from analysis of crystallographic data by De Ridder et al.²¹ and one recently noticed by Zou and Brown.²² De Ridder et al.²¹ described this positive correlation as an “inverse” trans effect—reciprocal to the normal correlation—in which one bond shortens while the other lengthens, as in the case of XO [$\text{X} = \text{O}, \text{C}$ or N] ligands binding to heme.²³ According to our calculations each trans ligand (Im, DBI or H_2O) produces a straight line with a positive slope and regardless of its basicity, the $\text{Co}-\text{C}_\text{R}$ and $\text{Co}-\text{N}_\text{B}$ bonds either lengthen or shorten together (Tables 1–3; Figure 3). The slopes for DBI and H_2O are almost identical and equal to 1.935 and 1.930 respectively, while the slope for Im is slightly lower and is equal to 1.297. The stronger the basic character of the trans ligand ($\text{Im} > \text{DBI} > \text{H}_2\text{O}$), the stronger the bond it forms with the Co atom. Further strengthening of this bond is achieved by formation of a hydrogen bond as we demonstrated by optimizing the structure of $\text{Im}-[\text{Co}^{\text{III}}(\text{corrin})]-\text{Me}$ with a water molecule attached to the imidazole. Bonding of water shortens the $\text{Co}-\text{N}_\text{B}$ bond by about ~ 0.02 Å (Table 1, Figure 3). The unconstrained geometry optimization of $\text{B}-[\text{Co}^{\text{III}}(\text{corrin})]-\text{R}$ shows that for certain combinations of axial ligands (B,R), like ($\text{H}_2\text{O}, \text{iProp}$), ($\text{H}_2\text{O}, \text{tBut}$), (DBI, iProp), (DBI, tBut) or (Im, tBut), the trans axial base (B) is not part of the Co coordination sphere (Figure 3). The open symbols represent the situation where the cobalt atom is no longer in the corrin plane and is displaced at least 0.10 Å above the average plane towards the alkyl R group, as is summarized in Figure 4. We adopted this criteria based on analysis of optimized structures of $[\text{Co}^{\text{III}}(\text{corrin})]-\text{R}$ ($\text{R} = \text{iProp}$ or tBut) without trans axial base. The increased complexity of R consequently leads to a flatter potential energy surface for the $\text{Co}-\text{N}_\text{B}$ stretch and in the case of $\text{R} = \text{tBut}$ does not lead to a stable minimum at

TABLE 1: Selected DFT Optimized Bond Lengths (Å) of Im-[Co^{III}-corrin]-R Compared with Available Experimental Data

	Im-[Co ^{III} -corrin]-R ^a							experiment Coβ-cyano- imidazylcobamid ^c
	-CN	-CCH	-Me	-Et	-Ado	-iProp	-tBut	
Co-N1	1.904	1.902	1.894 (1.895) ^b	1.894	1.897	1.892	1.895	1.835
Co-N2	1.950	1.949	1.945 (1.945)	1.947	1.950	1.949	1.946	1.899
Co-N3	1.951	1.950	1.946 (1.946)	1.943	1.940	1.945	1.947	1.853
Co-N4	1.895	1.892	1.890 (1.890)	1.891	1.893	1.891	1.896	1.880
Co-C _R	1.873	1.871	1.962 (1.964)	1.989	1.994	2.033	2.103	1.863
Co-N _B	2.090	2.115	2.218 (2.196)	2.261	2.222	2.325	2.418	1.968

^a Present work, nonlocal DFT with B3LYP functional. ^b B = H₂O...Im. ^c Reference 16.

TABLE 2: Selected DFT Optimized Bond Lengths (Å) of DBI-[Co^{III}-corrin]-R Compared with Available Experimental Data

	DBI-[Co ^{III} -corrin]-R ^a						experiment MeB ₁₂ ^d
	-CN	-Me	-Et	-iProp	-tBut	vitamin B ₁₂ wet ^b (dry) ^c	
Co-N1	1.894	1.889	1.890	1.889	1.890	1.80 (1.86)	1.88
Co-N2	1.952	1.946	1.942	1.943	1.937	1.92 (1.89)	1.97
Co-N3	1.946	1.941	1.942	1.941	1.943	1.86 (1.91)	1.93
Co-N4	1.902	1.892	1.889	1.888	1.894	1.87 (1.95)	1.89
Co-C _R	1.871	1.962	1.990	2.027	2.091	1.92 (2.02)	1.99
Co-N _B	2.125	2.293	2.358	2.586	2.841	1.97 (2.06)	2.19

^a Present work, nonlocal DFT with B3LYP functional. ^b Reference 17. ^c Reference 18. ^d Reference 19

TABLE 3: Selected DFT Optimized Bond Lengths (Å) of H₂O-[Co^{III}-corrin]-R

	H ₂ O-[Co ^{III} -corrin]-R ^a				
	-CN	-Me	-Et	-iProp	-tBut
Co-N1	1.887	1.887	1.887	1.891	1.893
Co-N2	1.945	1.940	1.943	1.943	1.943
Co-N3	1.946	1.940	1.938	1.937	1.944
Co-N4	1.895	1.885	1.887	1.888	1.895
Co-C _R	1.846	1.948	1.975	2.015	2.083
Co-O	2.159	2.321	2.378	2.500	2.672

^a Present work, nonlocal DFT with the B3LYP functional.

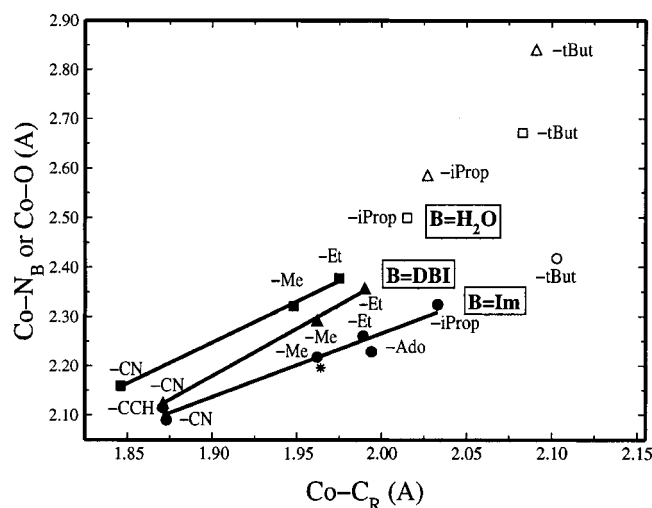


Figure 3. Plot of DFT-optimized Co-N vs Co-C_R bond lengths. Symbols: ●, B = Im [* : B = Im...H₂O, R = Me]; ▲, B = DBI [Δ, B = DBI not part of the Co coordination sphere]; ■, B = H₂O [□, B = H₂O not part of the Co coordination sphere]. Slopes and correlation coefficients (s, r): B = Im (1.297, 0.980); B = DBI (1.935, 0.999); B = H₂O (1.930, 0.999).

all. We may note that the linear correlation of the points for a given base has only a limited extent and is valid in the range of 1.85 – 2.00 Å for Co-C_R bond distance and is related to the nature of trans ligand (Figure 3).

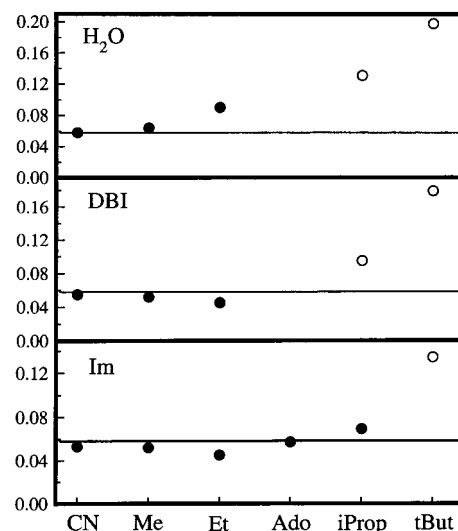


Figure 4. Cobalt out-of-plane displacement as a function of alkyl group R in model cobalamines B-[Co^{III}(corrin)]-R.

Variation of the trans ligand has also little effect on the Co-C_R bond length. The Co-C_R bond length varies only 0.002 Å (on average) when DBI base is replaced by Im (Tables 1 and 2, Figure 3). This observation is consistent with conclusions based on spectroscopic evidence by Spiro and co-workers²⁵ that Co-C_R stretching frequencies reflect bond strength in alkyl cobalamins, but are unaffected by trans ligand substitution. Contrary to the conclusions reached in this paragraph Marynick and co-workers^{11b} obtained different correlations between the Co-C_R and Co-N_B bond lengths. They also carried out a study of the geometric structure of Co(corrin)(L)(R)⁺ using the partial retention of diatomic differential overlap (PRDDO/M) molecular orbital technique. Their optimized geometries of nine corrin derivatives with axial ligands of varying degrees of steric bulkiness (R = Me, iProp, Ado; L = NH₃, pyridine, DBI) correlate differently than ours. They found that as the steric bulkiness of the alkyl ligand increases slightly, the Co-N_B bond distance tends to decrease. The latter trend does not hold for the sterically unhindered -NH₃ derivatives for which the Co-N distance is in the range 2.22–2.23 Å. We believe that this difference is due to the simplified character of their calculations.

The simultaneous elongation of the Co-C_R and Co-N_B bonds is inherently coupled to the conformational change of the corrin macrocycle ring. This conformational change is measured by eight torsional angles, defined according to the convention used in the Gaussian98 program,¹⁵ and is summarized in Figures 5–8. For clarity of presentation we abbreviated each torsional angle as [Co-N_x-C_y] defined with respect to the opposite nitrogen in the Co[N]₄ average plane in order to emphasize the existing C₂ pseudo-symmetry among them (Figure 5 and Figures 6–8). Conformational change of each pyrrolinyl group (A, B, C and D) is described by two torsional

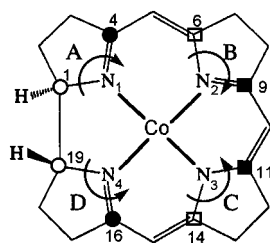


Figure 5. Pictorial description of the distortion of the corrin macrocycle ring. Open and filled symbols indicate displacements above and below the plane of the figure. Common shape of symbols for A, D (●, ○) and B, C rings (■, □) indicate C_2 pseudo-symmetry of the corrin macrocycle ring.

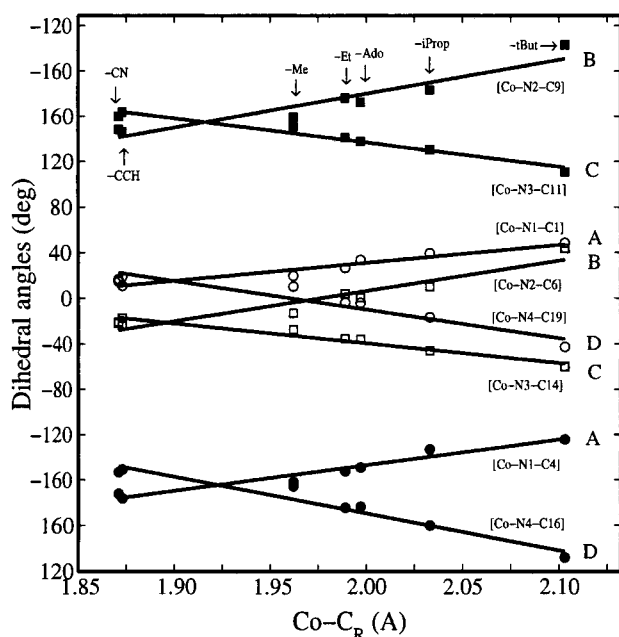


Figure 6. Plot of DFT-optimized $\text{Co}-\text{C}_R$ bond lengths vs dihedral angles describing distortion of the corrin ring in $\text{DBI}-[\text{Co}^{\text{III}}\text{-corrin}]-\text{R}$ model complexes. Labels and symbols follow Figures 2 and 5.

angles which follow a straight line as the inter-ligand bond elongates. This is qualitatively a new type of distortion which previously has not been reported, most likely because crystal structures of cobalamins are frequently disordered and inaccurate as can be judged from the crystallographic reliability indices.²⁰ This distortion can be pictured as a swivel of pyrrolinyl groups with respect to the corrin average plane and the corrin ring essentially flattens as the $\text{Co}-\text{C}_R$ bond elongates. Reduction of eight dihedral angles to a single quantity was unsuccessful, though it has been known for a long time^{6a} that a preferred mode of deformation of the corrin ring [i.e. upward folding] is a folding about an axis approximately bisecting the C_1-C_{19} bond and passing through atom C_{10} (see Figure 2). This deformation is measured by a “fold angle” defined as the dihedral angle between best fit planes through rings A + B and rings C + D, respectively. To further investigate the nature of the calculated conformational distortion, we fitted optimized Cartesian coordinates to a single fold angle defined according to Glusker and co-workers.^{6b} We found that each trans ligand produced a straight line with negative slope (Figure 9). However, the accuracy of the least-squares fit for the fold angle is only about 0.62 (for $\text{B} = \text{Im}$), while for pyrrolinyl swivel (Figure 5) it is about 0.96. Although the fold angle represents a conceptually simpler quantity, the conformational distortion is much more accurately described by eight torsional angles and we conclude

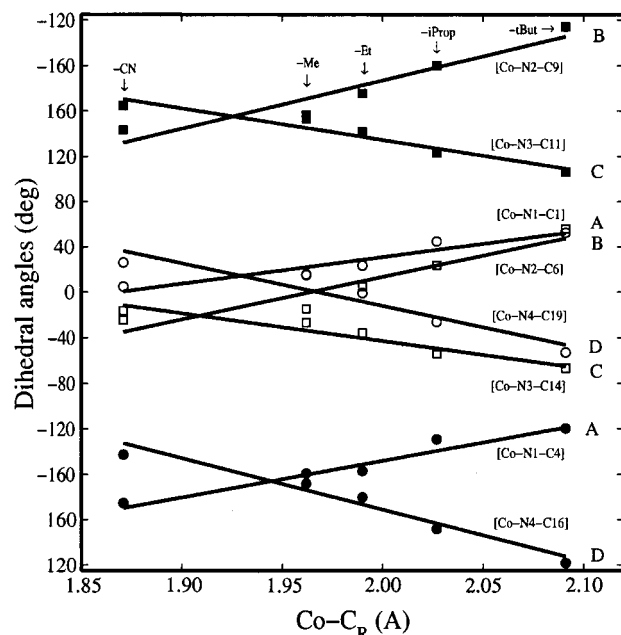


Figure 7. Plot of DFT-optimized $\text{Co}-\text{C}_R$ bond lengths vs dihedral angles describing distortion of the corrin ring in $\text{DBI}-[\text{Co}^{\text{III}}\text{-corrin}]-\text{R}$ model complexes. Labels and symbols follow Figures 2 and 5.

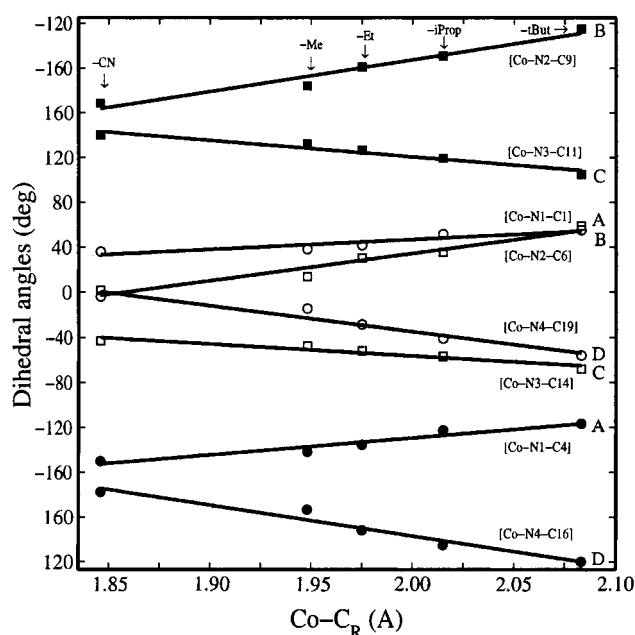


Figure 8. Plot of DFT-optimized $\text{Co}-\text{C}_R$ bond lengths vs dihedral angles describing distortion of the corrin ring in $\text{H}_2\text{O}-[\text{Co}^{\text{III}}\text{-corrin}]-\text{R}$ model complexes. Labels and symbols follow Figures 2 and 5.

that the pyrrolinyl swivel can be considered as a more physical quantity than the fold angle.

The positive correlation between the $\text{Co}-\text{C}_R$ and $\text{Co}-\text{N}_B$ bond lengths and simultaneous flattening of the corrin ring can only be explained on the basis of electronic considerations. The steric bulk of the B and R ligands cannot be considered as a determining factor in why the $\text{Co}-\text{C}_R$ and $\text{Co}-\text{N}_B$ bonds correlate positively. For a given R group, the $\text{Co}-\text{N}_B$ bond is longer for sterically less bulky water (H_2O) than for dimethylbenzimidazole (DBI) and the increase in the $\text{Co}-\text{N}_B$ bond length is in the order $\text{H}_2\text{O} > \text{DBI} > \text{Im}$ (Figure 3). For a given trans ligand (B) the $\text{Co}-\text{C}_R$ bond length for $-\text{Ado}$ is between $\text{R} = -\text{Et}$ and $\text{R} = -\text{iProp}$ (Figure 3). If the steric interaction were mainly responsible for a positive correlation between the $\text{Co}-$

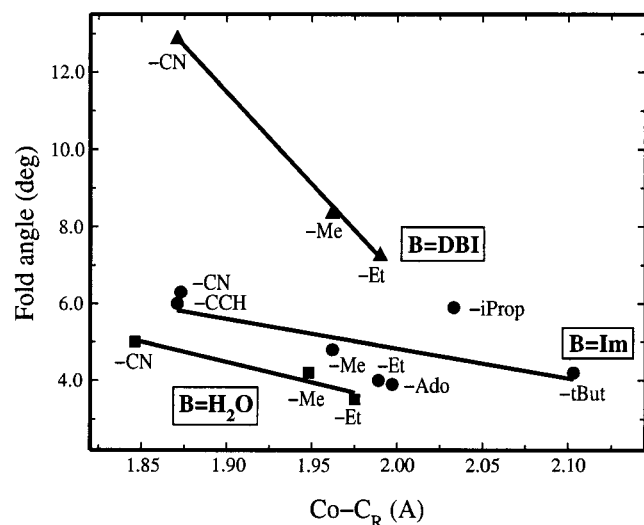


Figure 9. Fold angles for B-[Co^{III}-corrin]-R complexes. Symbols: ●, B = Im; ▲, B = DBI; ■, B = H₂O. Slopes and correlation coefficients (*s*, *r*): B = Im (-7.711, -0.624); B = DBI (-47.649, -0.999); B = H₂O (-10.585, -0.959).

TABLE 4: Selected DFT Optimized Bond Angles (deg) of DBI-[Co^{III}-corrin]-R Compared with Available Experimental Data

	DBI-[Co ^{III} -corrin]-R ^a		experiment	
	-CN	-Me	vitamin B ₁₂ wet ^b (dry) ^c	MeB ₁₂ ^d
N1-Co-N2	91.4	91.2	89 (91)	93
N1-Co-N3	173.5	173.0	175 (174)	172
N1-Co-N4	82.5	82.5	84 (81)	81
N1-Co-C _R	91.1	93.1	87 (89)	95
N2-Co-N3	94.9	95.1	96 (94)	95
N2-Co-N4	172.0	172.9	171 (170)	173
N2-Co-C _R	87.6	87.2	87 (87)	86
N3-Co-N4	91.3	91.4	92 (94)	90
N3-Co-C _R	90.4	90.2	91 (90)	87
N4-Co-C _R	87.4	89.9	89 (87)	90
N1-Co-N _B	90.0	88.9	96 (94)	93
N2-Co-N _B	93.2	92.2	88 (90)	89
N3-Co-N _B	88.4	90.2	87 (88)	86
N4-Co-N _B	91.9	90.9	97 (97)	95
C _R -Co-N _B	178.7	177.9	174 (175)	171

^a Present work, nonlocal DFT with B3LYP functional. ^b Reference 17. ^c Reference 18. ^d Reference 19.

C_R and Co-N_B bonds, one might expect that stretching of the Co-N_B bond would automatically lengthen the Co-C_R bond. Elongation of the Co-N_B bond does not influence the Co-C_R bond nor does angular deformation of the R ligand with respect to the corrin ring, as has been verified by our calculations. We carried out geometry optimization of Im-[Co^{III}-corrin]-Me or Et, with a constraint imposed on the angular deformation of the -R group with respect to corrin ring. In the case of Im-[Co^{III}-corrin]-Me we tilted the Co-Me group by constraining the N[Im]-Co-Me angle to 170° and 160°, while for Im-[Co^{III}-corrin]-Et we constrained the bent Co-C-C[Et] angle to 130°. In both cases the Co-C_R bond length remained unchanged, i.e., 1.962 Å for Me and 1.988 Å for Et (see Table 1 for comparison).

We further investigated the assertion that electronic effects cause changes in the Co-C_R and Co-N_B bonds by substitution of electron-donating and -withdrawing groups in an alkyl ligand (Table 5, Figure 10). As the R ligand becomes more electron-withdrawing, the Co-C_R bond length changes little (0.008 Å in average, Table 5), but the Co-N_B bond shortens approximately about 0.101 Å. Withdrawal of electrons from the

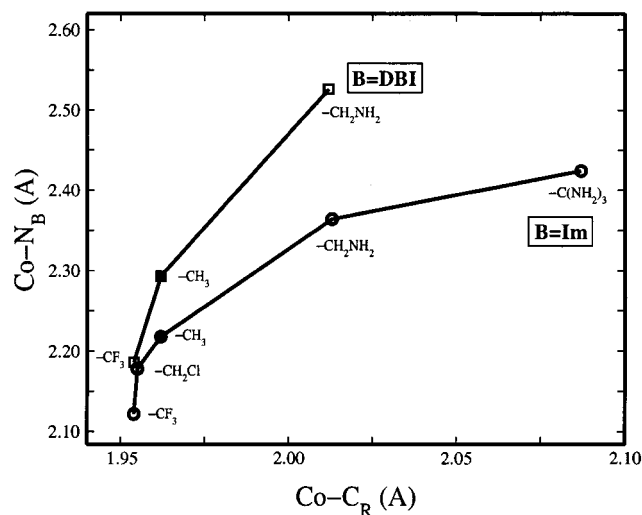


Figure 10. Plot of DFT-optimized Co-N_B vs Co-C_R bond lengths in Im-[Co^{III}-corrin]-R and DBI-[Co^{III}-corrin]-R model complexes. Symbols: ●, R = CH₃, B = Im; ■, R = CH₃, B = DBI; ○, R replaced by electron-donating [-CH₂NH₂, -C(NH₂)₃] or -withdrawing [-CH₂-Cl, -CF₃] group, B = Im; □, R replaced by electron-donating [-CH₂-NH₂] or -withdrawing [-CH₂-Cl, -CF₃] group, B = DBI.

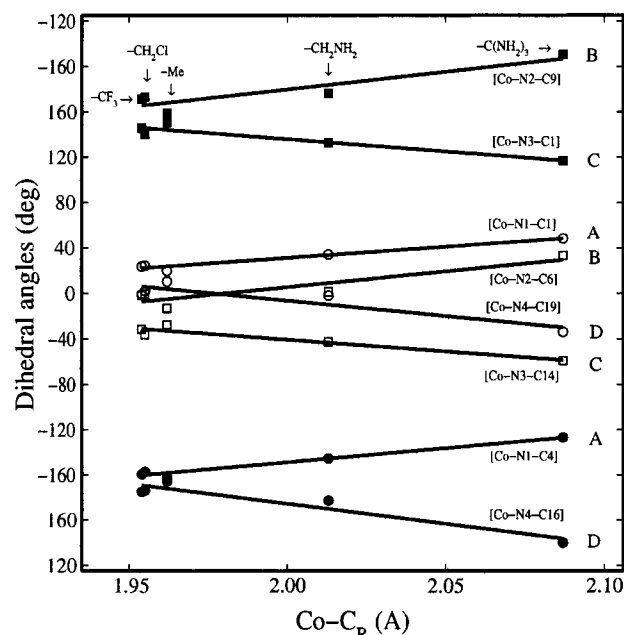
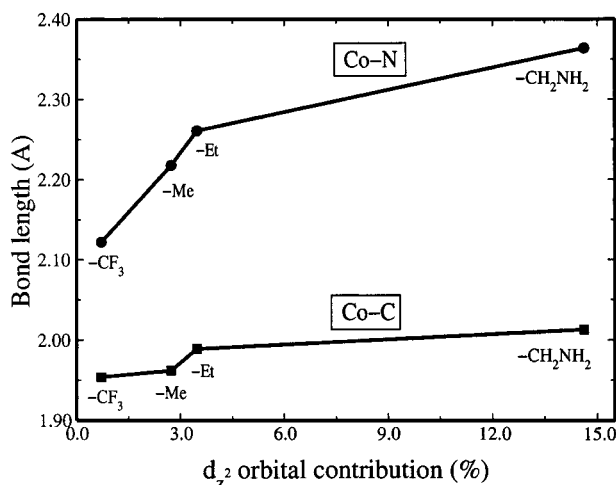


Figure 11. Plot of DFT-optimized Co-C_R bond lengths vs dihedral angles describing distortion of the corrin ring in Im-[Co^{III}-corrin]-R model complexes, where R = CF₃, CH₂Cl, CH₃, CH₂NH₂ and C(NH₂)₃. Labels and symbols follow Figures 2 and 5.

d_{z² orbital of Co strongly affects the donor-acceptor character of the Co-N_B bond but leaves the covalent bond intact. On the other hand, donation of electrons leads to a simultaneous elongation of the Co-C_R and Co-N_B bonds and a conformational change of the corrin ring as shown in Figures 10 and 11. This result may be paraphrased by saying that population of the d_{z² orbital of Co controls the Co-C_R/Co-N_B distances as it shown for the HOMO orbital in Figure 12. The correlation between the Co-C_R/Co-N_B bond lengths and the d_{z² occupation of the HOMO shows that -Me group participation of the d_{z² is roughly about 3% and is less than 1% when -Me is replaced by -CF₃. However, when one hydrogen in -Me is replaced by an -NH₂ group, the contribution of d_{z² increases to 15% (Figure 12). Replacement of all three hydrogens in -Me by}}}}}

TABLE 5: Selected DFT Optimized Bond Lengths (Å) of Im-[Co^{III}-corrin]-R and DBI-[Co^{III}-corrin]-R Compared with Available Experimental Data

	Im-[Co ^{III} -corrin]-R ^a					DBI-[Co ^{III} -corrin]-R ^a			experiment -CF ₃ B ₁₂ ^b
	-CF ₃	-CH ₂ Cl	-CH ₃	-CH ₂ NH ₂	-C(NH ₂) ₃	-CF ₃	-CH ₃	-CH ₂ NH ₂	
Co-N1	1.902	1.898	1.894	1.888	1.894	1.899	1.889	1.884	1.870
Co-N2	1.948	1.940	1.945	1.942	1.955	1.941	1.946	1.936	1.951
Co-N3	1.944	1.942	1.946	1.949	1.941	1.943	1.941	1.946	1.887
Co-N4	1.894	1.895	1.890	1.889	1.891	1.892	1.892	1.886	1.917
Co-C _R	1.954	1.955	1.962	2.013	2.087	1.954	1.962	2.012	1.878
Co-N _B	2.122	2.178	2.218	2.364	2.424	2.186	2.293	2.526	2.047

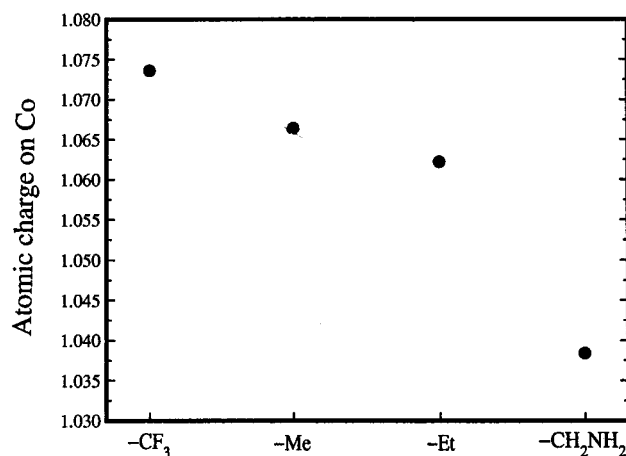
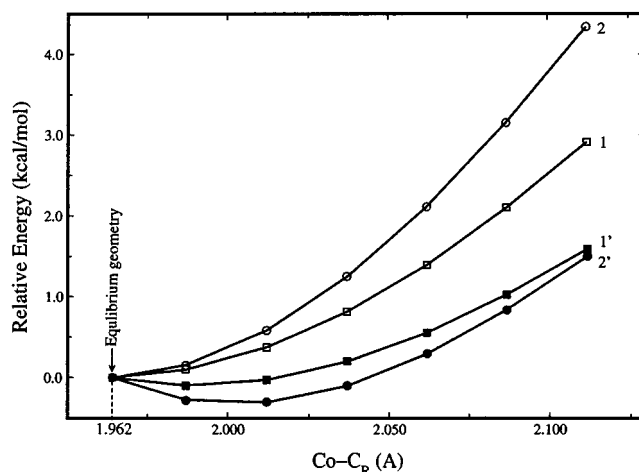
^a Present work, nonlocal DFT with B3LYP functional. ^b Reference 22.**Figure 12.** Correlation between the Co-C_R/Co-N_B bond lengths and the d₂ occupation of the HOMO orbital in Im-[Co^{III}-corrin]-Me.

-NH₂ has an even more dramatic impact and the Co-C_R bond can easily increase by more than 0.1 Å as shown in Figure 10.

Conclusions and Summary

The most important conclusions from this work are the positive correlation between the Co-C_R and Co-N_B bond lengths for a given base B (Figure 3) and the fact that electron donation from axial R ligands to the cobalt atom by electron donating substituents is mainly responsible for labilization of the Co-C_R bond (Figure 10). This positive correlation is attributed to one common phenomena: the charge on Co. More electronegative R substituents will tend to have shorter Co-C_R bonds because of both σ and π effects and, by withdrawing charge from Co, will tend to reduce the Co-N_B bond. To support this conclusion we calculated atomic charges on Co, as is shown in Figure 13. These calculations show two interesting points: 1) the charge on Co decreases in the order -CF₃ > -Me > -Et > -CH₂NH₂, and 2) the cobalt in six-coordinate cobalamin models looks more like Co^I rather than Co^{III}. The latter shows that axial ligands only slightly perturb the four coordinate corrin moiety.

In light of the present DFT calculations the steric mechanism, including the Co-N_B bond elongation or angular distortion, cannot be considered as the initial trigger for Co-C_R bond activation in coenzyme B₁₂ as has frequently been suggested.^{4c,7b} The initial activation of the Co-C_R bond can be understood only on the basis of electronic considerations. More specifically, when the coenzyme is embedded in a protein matrix, the electrostatic field generated by polar aminoacids of the protein is capable of facilitating electron reorganization in the N_B-Co-C_R moiety and consequently leads to labilization of the Co-C_R bond. To support this statement we carried out model calculations on methyl cobalamin Im-[Co^{III}-corrin]-Me in the

**Figure 13.** Charge on cobalt out-of-plane a function of alkyl group R in model cobalamines Im-[Co^{III}(corrin)]-R.**Figure 14.** Relative energies of the methyl cobalamin Im-[Co^{III}-corrin]-Me model complex computed as a function of the Co-C_R and Co-N_B interligand distances in the presence (curves 1' and 2'; filled symbols ●, ■) and absence (curves 1 and 2; open symbols ○, □) of unit negative extend charge. Curves (1, 1'; squares) correspond to elongation of the Co-C_R bond alone, while (2, 2'; circles) correspond to simultaneous elongation of both C-C_R and Co-N_B bonds according to linear positive correlation (Figure 3).

presence and absence of an external negative charge placed 3.0 Å above the Co atom along the Co-C_R bond. The results of those calculations are summarized in Figure 14. Energy curves for Im-[Co^{III}-corrin]-Me in the presence of an external electric field exhibit minima, while those without a field increase systematically with elongation of the Co-C_R bond. Simultaneous elongation of two of the interligand bonds, Co-C_R and Co-N_B, further lowers the relative energy and the energy curve shows a shallow minimum. On the other hand stretching the two bonds simultaneously without an external field is more energetically costly than stretching only the Co-C_R bond. Thus,

two important factors are necessary: presence of external electric field and cooperativity between the Co–C_R and Co–N_B interligand bonds. Consequently, as the Co–C_R and Co–N_B bonds elongate, the nonequilibrium geometry could result in an angular strain or tensile force on the corrin. Whether this elongated bond further weakens depends on the presence or absence of steric hindrances between the Co–R group and the surrounding protein.

Acknowledgment. The authors thank Dr. G. Lamm for helpful discussions and a referee for clarifying suggestions. Issued as NRCC No. 43853.

Supporting Information Available: Tables of DFT-optimized bond distances, bond angles and dihedral angles, optimized Cartesian coordinates and energies for B–[Co^{III}, corrin]–R model complexes. This material is available free of charge via the Internet at <http://pubs.acs.org>.

References and Notes

- (1) (a) Dolphin, D., Ed. *B₁₂*; Wiley-Interscience: New York, 1982. (b) Kräutler, B.; Arigoni, D.; Golding, B. T., Eds.; *Vitamin B₁₂ and B₁₂ Proteins*; Wiley-VCH: New York, 1998.
- (2) Hay, B. P.; Finke, R. G. *J. Am. Chem. Soc.* **1986**, *108*, 4820.
- (3) (a) Hay, B. P.; Finke, R. G. *J. Am. Chem. Soc.* **1987**, *109*, 8012. (b) Finke, R. G.; Martin, B. D. *Inorg. Biochem.* **1990**, *40*, 19. (c) Garr, C. D.; Sirovatka, J. M.; Finke, R. G. *J. Am. Chem. Soc.* **1996**, *118*, 11142. (d) Sirovatka, J. M.; Finke, R. G. *J. Am. Chem. Soc.* **1997**, *119*, 3057.
- (4) (a) Pratt, J. M. In *B₁₂*; Dolphin, D., Ed.; Wiley-Interscience: New York, 1982; Vol. 1, Chapter 10. (b) Golding, B. T. In *B₁₂*; Dolphin, D., Ed.; Wiley-Interscience: New York, 1982; Vol. 1, Chapter 15. (c) Marzilli, L. G. In *Bioinorganic Catalysis*; Reedijk, J., Ed.; Marcel Dekker: New York, 1993; Chapter 8.
- (5) Randaccio, L.; Bresciani Pahor, N.; Zangrando, E.; Marzilli, L. G. *Chem. Soc. Rev.* **1989**, *18*, 225.
- (6) (a) Halpern, J. *Science* **1985**, *227*, 869. (b) Pett, V. B.; Liebman, M. N.; Murray-Rust, P.; Prasad, K.; Glusker, J. P. *J. Am. Chem. Soc.* **1987**, *109*, 9, 3207. (c) Kräutler, B.; Konrat, R.; Stupperich, E.; Farber, G.; Gruber, K.; Kratky, C. *Inorg. Chem.* **1994**, *33*, 4128.
- (7) (a) Pratt, J. M. *Chem. Soc. Rev.* **1985**, 161–170. (b) Zhu, L.; Kostic, N. M. *Inorg. Chem.* **1987**, *26*, 4194.
- (8) (a) Mealli, C.; Sabat, M.; Marzilli, L. G. *J. Am. Chem. Soc.* **1987**, *109*, 1593. (b) Evans, P. R.; Mancia, F. in *Vitamin B₁₂ and B₁₂-Proteins*; Kräutler, B., Arigoni, D., Golding, B. T., Eds.; Wiley-VCH: New York, 1998; Chapter 13.
- (9) Spiro, T. G.; Kozlowski, P. M.; Zgierski, M. Z. *J. Raman. Spectrosc.* **1998**, *29*, 869.
- (10) (a) Salem, L.; Eisenstein, O.; Anh, N. T.; Burgi, H. B.; Devaquet, A.; Segal, A.; Veillard, A. *Nouv. J. Chim.* **1977**, *1*, 335. (b) Christianson, D. W.; Lipscomb, W. N. *J. Am. Chem. Soc.* **1985**, *107*, 2682.
- (11) (a) Hansen, L. M.; Pavan-Kumar, P. N. V.; Marynick, D. S. *Inorg. Chem.* **1994**, *33*, 728. (b) Hansen, L. M.; Derecskei-Kovacs, A.; Marynick, D. S. *J. Mol. Struct. (THEOCHEM)*, **1998**, *431*, 53.
- (12) Andruniow, T.; Zgierski, M. Z.; Kozlowski, P. M. *Chem. Phys. Lett.*, in press (2000).
- (13) Schaefer, A.; Horn, H.; Ahlrichs, R. *J. Chem. Phys.* **1992**, *97*, 2571.
- (14) (a) Kozlowski, P. M.; Spiro, T. G.; Berces, A.; Zgierski, M. Z. *J. Phys. Chem. B* **1998**, *102*, 2603. (b) Kozlowski, P. M.; Rush, T. S., III; Jarzecki, A. A.; Zgierski, M. Z.; Chase, B.; Piffat, C.; Ye, B.-H.; Li, X.-Y.; Pulay, P.; Spiro, T. G. *J. Phys. Chem. A* **1999**, *103*, 1357. (c) Spiro, T. G.; Kozlowski, P. M. *J. Am. Chem. Soc.* **1998**, *120*, 4524.
- (15) (a) Frisch, M. J.; Frisch, M. J.; Trucks, G. W.; Schlegel, H. B.; Scuseria, G. E.; Robb, M. A.; Cheeseman, J. R.; Zakrzewski, V. G.; Montgomery, J. A., Jr.; Stratmann, R. E.; Burant, J. C.; Dapprich, S.; Millam, J. M.; Daniels, A. D.; Kudin, K. N.; Strain, M. C.; Farkas, O.; Tomasi, J.; Barone, V.; Cossi, M.; Cammi, R.; Mennucci, B.; Pomelli, C.; Adamo, C.; Clifford, S.; Ochterski, J.; Petersson, G. A.; Ayala, P. Y.; Cui, Q.; Morokuma, K.; Malick, D. K.; Rabuck, A. D.; Raghavachari, K.; Foresman, J. B.; Cioslowski, J.; Ortiz, J. V.; Stefanov, B. B.; Liu, G.; Liashenko, A.; Piskorz, P.; Komaromi, I.; Gomperts, R.; Martin, R. L.; Fox, D. J.; Keith, T.; Al-Laham, M. A.; Peng, C. Y.; Nanayakkara, A.; Gonzalez, C.; Challacombe, M.; Johnson, P. B.; Chen, W.; Wong, M. W.; Andres, J. L.; Gonzalez, C.; Head-Gordon, M.; Replogle, E. S.; Pople, J. A. *Gaussian 98*, Revision A.3; Gaussian, Inc.: Pittsburgh, PA, 1998. (b) PQS, version 2.2: Parallel Quantum Solutions, 2013 Green Acres Road, Fayetteville, AR 72703, USA, 1999 (<http://www.pqs-chem.com>).
- (16) Kräutler, B.; Konrat, R.; Stupperich, E.; Färber, G.; Gruber, K.; Kratky, C. *Inorg. Chem.* **1994**, *33*, 4128.
- (17) Brink-Shoemaker, C.; Cruickshank, D. W. J.; Hodgkin, D. C.; Kamper, M. J.; Pilling, D. *Proc. R. Soc. London, Ser. A* **1964**, *278*, 1.
- (18) Hodgkin, D. C.; Lindsey, J.; Sparks, R. A.; Trueblood, K. N.; White, J. G. *Proc. R. Soc. London, Ser. A* **1962**, *266*, 494.
- (19) Rossi, M.; Glusker, J. P.; Randaccio, L.; Summers, M. F.; Toscano, P. J.; Marzilli, L. G. *J. Am. Chem. Soc.* **1985**, *107*, 1729.
- (20) Gruber, K.; Jögl, G.; Klintschar, G.; Kratky, C. In *Vitamin B₁₂ and B₁₂-Proteins*; Kräutler, B., Arigoni, D., Golding, B. T., Dolphin, D., Eds.; Wiley-VCH: New York, 1998; Chapter 22.
- (21) De Ridder, D. J. A.; Zangrando, E.; Bürgi, H.-B. *J. Mol. Struct.* **1996**, *374*, 63.
- (22) Zou, X.; Brown, K. L. *Inorg. Chim. Acta* **1998**, *267*, 305.
- (23) Vogel, K. M.; Kozlowski, P. M.; Zgierski, M. Z.; Spiro, T. G. *J. Am. Chem. Soc.* **1999**, *121*, 9915.